Three-Dimensional Analysis of Harmonic Generation in Self-Amplified Spontaneous Emission

Zhirong Huang [1], Kwang-Je Kim

Advanced Photon Source, Argonne National Laboratory, Argonne, IL 60439, USA

Abstract

In a high-gain free-electron laser, strong bunching at the fundamental wavelength can drive substantial harmonic bunching and sizable power levels at the harmonic frequencies. In this paper, we investigate the three-dimensional evolution of the harmonic fields based on the coupled Maxwell-Vlasov equations that take into account the nonlinear harmonic interaction. Each harmonic field is the sum of a self-amplified term and a term driven by the nonlinear harmonic interaction. In the exponential gain regime, the growth rate of the dominant nonlinear term is much faster than that of the self-amplified harmonic field. As a result, the gain length and the transverse profile of the first few harmonics are completely determined by those of the fundamental. A percentage of the fundamental power level is found at the third harmonic frequency right before saturation for the current self-amplified spontaneous emission projects.

Key words: Harmonic generation; High-gain free-electron laser; Self-amplified spontaneous emission
PACS: 41.60.Cr; 42.55.Vc; 42.65.Ky

1 Introduction

In a planar wiggler, spontaneous emissions at the fundamental resonant frequency and its higher harmonics induce bunching at their respective wavelength scales, leading to amplified emissions [1]. Such a process is heavily in

[1] Corresponding author. Tel: (630)252-6023; Fax: (630)252-5703; Email: zrh@aps.anl.gov

DISCLAIMER

DISCLAIMER

Portions of this document may be illegible in electronic image products. Images are produced from the best available original document.

favor of the fundamental frequency and is the underlying principle for the design of the fourth-generation light sources [2,3]. However, a one-dimensional model [4] and a three-dimensional simulation study [5] indicate that strong bunching at the fundamental wavelength can also drive substantial harmonic bunching and sizable harmonics power. In this paper, we attempt to make a three-dimensional analysis of harmonic generation by taking into account the nonlinear harmonic interaction. Starting from the fundamental, we determine the dominant contribution to the first few harmonics. Explicit calculation based on the current self-amplified spontaneous emission (SASE) projects is used to demonstrate the characteristics of the third harmonic radiation.

2 The Coupled Maxwell-Vlasov System

For an electron in a planar wiggler (with the wiggler parameter K), the transverse wiggling motion is accompanied by a longitudinal oscillation (at twice the transverse frequency ck_w) about the average longitudinal motion z^*. This figure-eight motion (in the comoving frame) can give rise to harmonic emissions. In the forward z direction, the radiation field is a series of (nearly) monochromatic waves at odd harmonics ($h = 1, 3, 5, ...$) of the fundamental resonant frequency ck_1 [1], i.e.,

$$\mathbf{E} = \hat{x} \sum_h \left[\frac{1}{2} A_h(\mathbf{r}, z) e^{ihk_1(z-ct)} + \text{c. c.} \right], \tag{1}$$

where $\mathbf{r} = (x, y)$ represents the transverse coordinates and the field amplitude A_h is assumed to be varying slowly with z. In order to have a nonvanishing radiation at the h^{th} harmonic, the electron distribution function $f(\theta, \eta, \mathbf{r}, \mathbf{p}, z)$ must have a component with the $e^{ih\theta}$ dependence, where $\theta = (k_w + k_1)z^* - ck_1 t$ is the longitudinal phase coordinate, $\eta = (\gamma - \gamma_0)/\gamma_0$, and $\mathbf{p} = d\mathbf{r}/dz$ are the

conjugate variables to θ and $\mathbf{r}$. Using the Pierce parameter ρ [6], we introduce the following scaled variables:

$$\begin{aligned}\bar{z} =& 2\rho k_w z, \quad \bar{\eta} = \frac{\eta}{\rho},\\ \bar{\mathbf{r}} =& \mathbf{r}\sqrt{2k_1 k_w \rho}, \quad \bar{\mathbf{p}} = \mathbf{p}\sqrt{\frac{k_1}{2k_w\rho}},\end{aligned} \tag{2}$$

and the scaled field amplitude $a_h = \frac{eK_h A_h}{8\gamma_0^2 mc^2 k_w \rho^2}$, where

$$K_h = K(-1)^{(h-1)/2}[J_{(h-1)/2}(h\xi) - J_{(h+1)/2}(h\xi)]$$

with $\xi = K^2/(4+2K^2)$. The Maxwell-Vlasov equations can be written as [7]

$$\begin{aligned}&\left(\frac{\partial}{\partial\bar{z}} + \frac{\bar{\nabla}_\perp^2}{2ih}\right)a_h = \left(\frac{K_h}{K_1}\right)^2\left\langle e^{-ih\theta}\int d^2\bar{p}\int d\bar{\eta} f\right\rangle,\\ &f = f_0 + \int_0^{\bar{z}} d\bar{s}\sum_h e^{ih[\theta+\phi(\bar{s}-\bar{z})]}a_h(\bar{\mathbf{r}}',\bar{s})\\ &\qquad\times\frac{\partial}{\partial\bar{\eta}}f(\theta+\phi(\bar{s}-\bar{z}),\eta,\bar{\mathbf{r}}',\bar{\mathbf{p}}',\bar{s}),\end{aligned} \tag{3}$$

where $\phi = \bar{\eta} - (\bar{p}^2 + \bar{k}_n^2\bar{r}^2)/2$, $\bar{k}_n = K/(4\gamma_0\rho)$, and

$$\begin{aligned}\bar{\mathbf{r}}' =& \bar{\mathbf{r}}\cos(\bar{k}_n(\bar{s}-\bar{z})) + \frac{\bar{\mathbf{p}}}{\bar{k}_n}\sin(\bar{k}_n(\bar{s}-\bar{z})),\\ \bar{\mathbf{p}}' =& -\bar{k}_n\bar{\mathbf{r}}\sin(\bar{k}_n(\bar{s}-\bar{z})) + \bar{\mathbf{p}}\cos(\bar{k}_n(\bar{s}-\bar{z})).\end{aligned}$$

We have extended the summation of h to $-1,-3,-5,...$ to include the complex conjugate terms by introducing the notation $a_{-h} = -a_h^*$. The electron beam is assumed to be round and matched to the wiggler channel with a focusing strength $k_n = 2\rho k_w \bar{k}_n$ equally distributed in both transverse planes. The smooth part of the initial distribution function f_0 is modeled by

$$\frac{1}{2\pi\bar{\sigma}_r^2\bar{k}_n^2}\exp\left[-\frac{(\bar{p}^2+\bar{k}_n^2\bar{r}^2)}{2\bar{\sigma}_r^2\bar{k}_n^2}\right]\frac{e^{-\bar{\eta}^2/(2\bar{\sigma}_\eta^2)}}{\sqrt{2\pi}\bar{\sigma}_\eta}, \tag{4}$$

where $\bar{\sigma}_r$ and $\bar{\sigma}_\eta$ are the scaled beam size and scaled energy spread.

3 Harmonic Interaction

We solve Eq. (3) by a perturbation method. It is well known that the FEL reaches saturation [6] when $|a_1(r=0)|^2 \sim 1$. In the small signal regime before saturation, we postulate that

$$... < |a_h| < |a_{h-2}| < ... < |a_3| < |a_1| < 1. \tag{5}$$

We can then expand f in Eq. (3) as a power series of $\sum_h a_h e^{ih\theta}$. Collecting terms of arbitrary order in f that give an overall $e^{ih\theta}$ dependence (i.e., $\sum_m h_m = h$) and inserting them into the field part of Eq. (3), we obtain [7]

$$\begin{aligned}
&\left(\frac{\partial}{\partial \bar{z}} + \frac{\bar{\nabla}_\perp^2}{2ih}\right) a_h = \left(\frac{K_h}{K_1}\right)^2 \int d^2\bar{p} \int d\bar{\eta} \\
&\times \left[\int_0^{\bar{z}} d\bar{s}_1 e^{ih\phi\tau_1} a_h(\bar{\mathbf{r}}_1', \bar{s}_1) \frac{\partial f_0}{\partial \bar{\eta}} + \right. \\
&\quad \sum_{h_1+...+h_m=h} \int_0^{\bar{z}} d\bar{s}_1 e^{ih_1\phi\tau_1} a_{h_1}(\bar{\mathbf{r}}_1', \bar{s}_1) \frac{\partial}{\partial \bar{\eta}} \times ... \\
&\quad \left. \times \int_0^{\bar{s}_{m-1}} d\bar{s}_m e^{ih_m\phi\tau_m} a_{h_m}(\bar{\mathbf{r}}_m', \bar{s}) \frac{\partial f_0}{\partial \bar{\eta}} \right],
\end{aligned} \tag{6}$$

where $\tau_m = \bar{s}_m - \bar{s}_{m-1}$ for $m = 1, 2, 3, ...$ ($\bar{s}_0 = \bar{z}$), and $\bar{\mathbf{r}}_m' = \bar{\mathbf{r}} \cos(\bar{k}_n \tau_m) + \frac{\bar{\mathbf{p}}}{\bar{k}_n} \sin(\bar{k}_n \tau_m)$. The first term in the square bracket is the linear bunching due to the harmonic field itself, and the second term is the nonlinear bunching due to higher-order harmonic interaction. The general solution to Eq. (6) is in the form

$$a_h = a_h^L + a_h^{NL}, \tag{7}$$

where a_h^L is the solution to the homogeneous equation in the absence of the nonlinear terms, representing the self-amplified spontaneous emission, and a_h^{NL} is the particular solution that satisfies the inhomogeneous Eq. (6), representing the nonlinear harmonic interaction. Let $a_h^L = b_h^L(\bar{\mathbf{r}}) e^{\lambda_h \bar{z}}$ ($Re(\lambda_h) > 0$) be the

dominant mode with the largest growth rate. The dispersion relation for the complex eigenvalue λ_h and the transverse field profile b_h^L is similar to the one at the fundamental frequency [8]. The higher harmonics not only have lower coupling coefficients than the fundamental (i.e., $\left(\frac{K_h}{K_1}\right)^2 < 1$ for $h > 1$), but also suffer much worse warm-beam effects (energy spread and emittance) at shorter wavelength. Hence, we have $Re(\lambda_1) > Re(\lambda_{3,5,...})$, and the SASE process is predominantly the growth of the fundamental radiation power.

Nevertheless, significant power levels for the first few harmonics can still develop through nonlinear harmonic interaction. From Eq. (6), the order of the inhomogeneous solution is the same as the lowest-order terms of $a_{h_1} \times ... \times a_{h_m}$. For the fundamental radiation, we have $a_1^{NL} << a_1^L$ because of Eq. (5), and a_1 is guided by a single fastest-growing mode $b_1^L(\bar{\mathbf{r}})e^{\lambda_1 \bar{z}}$ in the exponential gain regime. At the third harmonic frequency, the leading nonlinear term is a_1^3, since any other combination such as $a_1 a_{-1} a_3$ or $a_1^4 a_{-1}$ is necessarily smaller due to Eq. (5). Assuming an effective noise level $1/\sqrt{N_c}$ for the fundamental and third harmonic emissions, we can write

$$a_3^L \sim \frac{1}{\sqrt{N_c}} e^{\lambda_3 \bar{z}}, \quad a_3^{NL} \sim a_1^3 \sim \left(\frac{1}{\sqrt{N_c}} e^{\lambda_1 \bar{z}}\right)^3.$$

If $Re(\lambda_3) << Re(\lambda_1)$, then we have

$$a_3 \approx \begin{cases} a_3^L, & \text{when} \quad \bar{z} < \frac{2}{3}\bar{z}_{sat} \\ a_3^{NL}, & \text{when} \quad \bar{z} > \frac{2}{3}\bar{z}_{sat}, \end{cases} \tag{8}$$

where $\bar{z}_{sat} \sim \frac{\ln N_c}{3Re(\lambda)}$ is the saturation length.

The equation for a_3^{NL} can be obtained from Eq. (6):

$$\left(\frac{\partial}{\partial\bar{z}}+\frac{\bar{\nabla}_\perp^2}{2ih}\right)a_3^{NL}=\left(\frac{K_3}{K_1}\right)^2\int d^2\bar{p}\int d\bar{\eta}$$
$$\times\left[\int_0^{\bar{z}}d\bar{s}_1e^{ih\phi_{T1}}a_3^{NL}(\bar{\mathbf{r}}',\bar{s})\frac{\partial f_0}{\partial\bar{\eta}}+\int_0^{\bar{z}}d\bar{s}_1e^{i\phi_{T1}}\right.$$
$$\times a_1(\bar{\mathbf{r}}_1',\bar{s})\frac{\partial}{\partial\bar{\eta}}\int_0^{\bar{s}_1}d\bar{s}_2e^{i\phi_{T2}}a_1(\bar{\mathbf{r}}_2',\bar{s}_2)\frac{\partial}{\partial\bar{\eta}}$$
$$\left.\times\int_0^{\bar{s}_2}d\bar{s}_3e^{i\phi_{T3}}a_1(\bar{\mathbf{r}}_3',\bar{s})\frac{\partial f_0}{\partial\bar{\eta}}\right]. \tag{9}$$

Thus, the radiation field at the third harmonic is completely driven by the third power of the fundamental field when $\bar{z}>\frac{2}{3}\bar{z}_{sat}$. As a result, both the growth rate and the transverse profile of the third harmonic radiation are completely determined by those of the fundamental. For the fifth harmonic, the leading nonlinear terms are $a_1^2a_3$ and a_1^5. Since a_3 is eventually dominated by a_1^3, both terms of a_5^{NL} are of the same order as a_1^5 and are the dominant components for a_5 after $\bar{z}>\frac{4}{5}\bar{z}_{sat}$. In general, the dominant nonlinear terms for a_h are of the same order as a_1^h, with a growth rate given by $h\lambda_1$. Such a growth rate scaling was pointed out for the third harmonic using a one-dimensional model [4] and was observed up to the ninth harmonic using a three-dimensional simulation code [5]. Here we present a three-dimensional analysis for this scaling by taking into account all possible harmonic interactions. The inequality of Eq. (5) we postulate is also consistent with the ordering of each harmonic. In passing, we note that this perturbation analysis is not valid when $\bar{z}$ is too close to z_{sat}.

4 Third Harmonic Radiation

The z-dependence of Eq. (9) can be explicitly factored out by writing $a_3^{NL}=b_3^{NL}(\bar{\mathbf{r}})e^{3\lambda_1\bar{z}}$ to obtain a transverse mode equation. Furthermore, we neglect the

first term in the square bracket because the linear-bunching effect is weak for any higher harmonics. Approximating the fundamental radiation profile by a Gaussian mode $b_1^L = b_0 \exp(-\bar{r}^2/w_1^2)$, we arrive at [7]

$$b_3^{NL}(\bar{r}) = 2\pi i \left(\frac{K_3}{K_1}\right)^2 b_0^3 \int_0^\infty \frac{q dq J_0(2\pi q\bar{r})\tilde{g}(q)}{3\lambda_1 + 2i\pi^2 q^2/3}, \tag{10}$$

where

$$\begin{aligned}\tilde{g} =& \frac{\pi w_1^4}{2\bar{\sigma}_r^2}\int_{-\infty}^0 d\tau_1 \int_{-\infty}^0 d\tau_2 \int_{-\infty}^0 d\tau_3 \tau_1(\tau_1+\tau_2) \\ & \times \frac{(\tau_1+\tau_2+\tau_3)}{T}\exp\left[-\frac{\bar{\sigma}_\eta^2}{2}(\tau_1+\tau_2+\tau_3)^2\right. \\ & \left. + \lambda_1(3\tau_1+2\tau_2+\tau_3) - \frac{\pi^2 q^2 w_1^2}{Q}\right],\end{aligned} \tag{11}$$

and

$$\begin{aligned}T =& \left[\sum_{m=1}^3 \sin^2(\bar{k}_n\tau_m)\right]\left[\sum_{m=1}^3 \cos^2(\bar{k}_n\tau_m)\right] \\ & - \left[\sum_{m=1}^3 \sin(\bar{k}_n\tau_m)\cos(\bar{k}_n\tau_m)\right]^2 + S^2 + 3S, \\ S =& \frac{w_1^2}{2\bar{\sigma}_r^2} + \frac{i}{2}\bar{k}_n^2\bar{\sigma}_r^2(\tau_1+\tau_2+\tau_3), \\ Q =& \frac{T}{S + \sum_{m=1,2,3}\sin^2(\bar{k}_n\tau_m)}.\end{aligned} \tag{12}$$

Since both λ_1 and w_1 are functions of $\bar{\sigma}_r$, $\bar{\sigma}_\eta$, and $\bar{k}_n$ [9], the transverse beam size of the third harmonic field is again a function of these three scaled parameters, determined by Eq. (10).

Using a quasi-fast Hankel transform algorithm [10], $b_3^{NL}(\bar{r})$ can be calculated numerically. For example, the initial stage of the low-energy undulator test line (LEUTL) FEL at the Advanced Photon Source [11] will use an electron beam with energy of 220 MeV, normalized emittance of 5π mm mrad, peak current of 150 A, energy spread of 0.1%. The external quadrupoles distribute the natural wiggler focusing equally in the horizontal and the vertical planes,

so that the average beta function is 1.5 m in both transverse planes. This yields $\bar{\sigma}_r = 0.56$, $\bar{\sigma}_\eta = 0.25$, and $\bar{k}_n = 0.46$. For the fundamental radiation at the optimal wavelength (around 520 nm), we find that $w_1/\bar{\sigma}_r = 2.6$ and $\lambda_1 = 0.5+0.1i$ [7]. Using these parameters, the normalized intensity of the third harmonic ($I_3 \equiv |b_3^{NL}(\bar{r})/b_3^{NL}(\bar{r}=0)|^2$) is obtained as shown in Fig. 1, with the optical waist given by $w_3/\bar{\sigma}_r = 1.4$ and the peak value $|b_3^{NL}(\bar{r}=0)|^2 = 0.17 b_0^6$. Integrating over the transverse cross section to obtain the third harmonic power P_3^{NL} from the nonlinear harmonic interaction, we obtain

$$\frac{P_3^{NL}}{\rho P_{\rm beam}} = 0.017 \left(\frac{P_1}{\rho P_{\rm beam}} \right)^3, \tag{13}$$

where P_1 is the FEL power at the fundamental frequency, and $P_{\rm beam}$ is the total beam power. Equation (13) is in good agreement with MEDUSA simulations [5] using a single-segmented wiggler. When P_1 approaches $\rho P_{\rm beam}$ just before saturation, the power in the third harmonic is a significant fraction (roughly 1%) of the power in the fundamental. A similar calculation yields a similar fractional power level for the third harmonic of the proposed LCLS project [2] (at 0.5 Å).

5 Conclusions

We have presented a perturbation method to analyze the harmonic radiation in self-amplified spontaneous emission, with explicit calculation of the third harmonic radiation based on the current SASE projects. In addition to other harmonic generation schemes proposed in the literature [12,13], the nonlinear harmonic interaction studied here could be a promising mechanism to generate coherent radiation at short wavelengths.

6 Acknowledgments

We wish to thank S. Biedron, H. Freund, and S. Milton for discussing their simulation results. This work was supported by the U. S. Department of Energy, Office of Basic Energy Sciences, under Contract No. W-31-109-ENG-38.

References

[1] W.B. Colson, IEEE J. Quantum Electron. **QE-17**, 1417 (1981).

[2] LCLS Design Study Report, SLAC-R-521, 1998.

[3] TESLA-FEL Conceptual Design, DESY 1997-048, 1997.

[4] R. Bonifacio *et al.*, Nucl. Instr. Meth. A **293**, 627 (1990).

[5] H.P. Freund *et al.*, submitted to IEEE J. Quantum Electron., and these proceedings.

[6] R. Bonifacio *et al.*, Opt. Comm. **50**, 373 (1984).

[7] Z. Huang and K.-J. Kim, in preparation.

[8] K.-J. Kim, Phys. Rev. Lett., **57**, 1871 (1986).

[9] L.-H. Yu *et al.*, Phys. Rev. Lett., **64**, 3011 (1990).

[10] A.E. Siegman, Opt. Lett., **1**, 13 (1977).

[11] S.V. Milton *et al.*, Nucl. Instr. Meth. A **407**, 210 (1998).

[12] R. Bonifacio *et al.*, Nucl. Instr. Meth. A **293**, 787 (1990).

[13] L.-H. Yu, Phys. Rev. A, **44**, 5178 (1991).

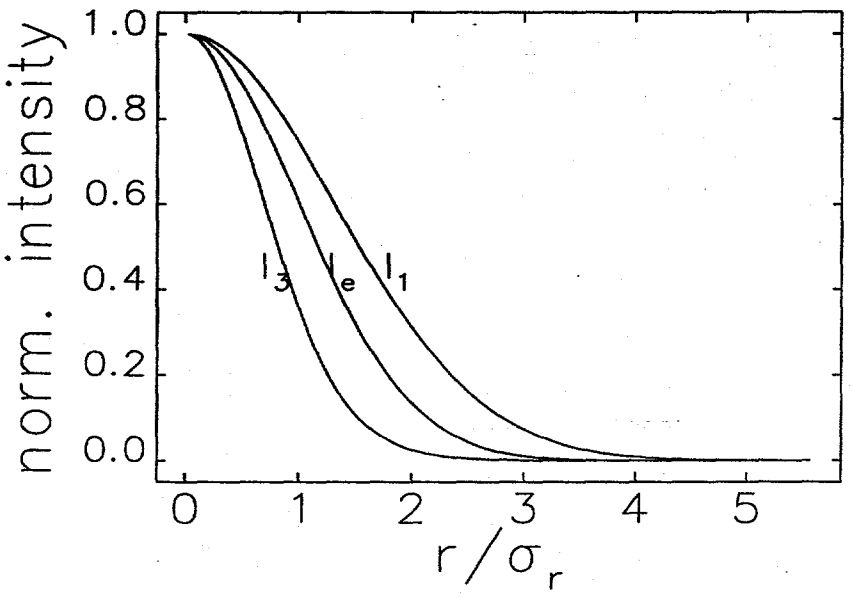

Fig. 1. The normalized intensity of the third harmonic (I_3), the electron beam (I_e), and the fundamental (I_1) as functions of the radius in units of the electron beam size, using the nominal LEUTL parameters.